Journal Pre-proof

Metformin alleviates oxidative stress and enhances autophagy in diabetic kidney disease via AMPK/SIRT1-FoxO1 pathway

Huiwen Ren, Ying Shao, Can Wu, Xiaoyu Ma, Chuan Lv, Qiuyue Wang

PII: S0303-7207(19)30330-2

DOI: https://doi.org/10.1016/j.mce.2019.110628

Reference: MCE 110628

To appear in: *Molecular and Cellular Endocrinology*

Received Date: 8 May 2019

Revised Date: 16 October 2019

Accepted Date: 17 October 2019

Please cite this article as: Ren, H., Shao, Y., Wu, C., Ma, X., Lv, C., Wang, Q., Metformin alleviates oxidative stress and enhances autophagy in diabetic kidney disease via AMPK/SIRT1-FoxO1 pathway, *Molecular and Cellular Endocrinology* (2019), doi: https://doi.org/10.1016/j.mce.2019.110628.

[Title page]

Metformin alleviates oxidative stress and enhances autophagy in diabetic kidney disease via AMPK/SIRT1-FoxO1 pathway

Huiwen Ren [1,2], Ying Shao [3], Can Wu [4], Xiaoyu Ma [5], Chuan Lv [6], Qiuyue Wang [1].*

1 Department of Endocrinology, the First Hospital Affiliated of China Medical University, Shenyang, Liaoning, China

2 Advanced Institute for Medical Sciences, Dalian Medical University, Dalian, Liaoning, China

3 Department of Endocrinology, the Second Hospital Affiliated of China Medical University, Shenyang, Liaoning, China

4 Department of Gastroenterology and Endoscopy, the First Hospital Affiliated of China Medical University, Shenyang, Liaoning, China

5 The Cadre Department, the First Hospital of China Medical University, Shenyang, Liaoning, China

6 Department of Endocrinology, the People's Hospital of Liaoning Province, Shenyang, Liaoning, China

[*] *Corresponding author: Qiuyue Wang*

Mailing address: The First Affiliated Hospital of China Medical University, 155 Nanjing North Street, Heping District, Shenyang 110001, Liaoning Province, China.

Email: wqycmu123@163.com

Telephone number: +86 024 83283135

Fax: 86 024 83283135

Running Title: Metformin with oxidative stress & autophagy in DKD

Keywords: Metformin; oxidative stress; autophagy; diabetic kidney disease

Word counts for the abstract: 149

Word counts for the main body of the text: 5087

Counts for figures: 8

Counts for tables: 1

[Highlights]

1. Metformin can ease glucose and lipid metabolism disorders, renal dysfunction and proteinuria in diabetic rats.

2. Metformin can relieve the oxidative stress response and promote autophagy in high glucose cultured rat mesangial cells.

3. The protective effect of metformin on diabetic kidney disease may be achieved through the AMPK/SIRT1-FoxO1 pathway.

Abstract

Metformin, as the basic pharmacological therapy and the first preventive drug in type 2 diabetes mellitus (T2DM), is proved to have potential protection in diabetic kidney disease (DKD). Here, we established a diabetic rat model induced by high-fat diet and low dose streptozotocin, and high glucose cultured rat mesangial cells (RMCs) pre-treated with metformin or transfected with AMPK, SIRT1 and FoxO1 small interfering RNA, and detected oxidative stress and autophagy related factors to explore the molecular mechanisms of metformin on DKD via adenosine monophosphate-activated protein kinase (AMPK)/silent mating type information regulation 2 homolog-1 (sirtuin-1, SIRT1)-Forkhead box protein O1 (FoxO1) pathway. We found that metformin effectively alleviated the disorders of glycolipid metabolism, renal function injury in diabetic rats, and relieved oxidative stress, enhanced autophagy and slowed down abnormal cell proliferation in high glucose cultured RMCs through AMPK/SIRT1-FoxO1 pathway, indicating the protective role of metformin against the pathological process of DKD.

Keywords: metformin; oxidative stress; autophagy; diabetic kidney disease

1. Introduction

Diabetes kidney disease (DKD), as one of the major microvascular complications of type 2 diabetes mellitus (T2DM) (Saran, Robinson, Abbott et al., 2018), is of great significance to reduce and delay the development of chronic kidney injury. Metformin, as the pharmacological therapy in T2DM patients, based on the latest guidelines of the American Diabetes Association 2018 edition, is proved to have long-term and short-term safety to prevent and delay diabetes (American Diabetes Association, 2018). Significant evidence exists that metformin can maintain the balance of glucose and lipid metabolism (De Jager, Kooy, Lehert et al., 2005,Di, Parborell, Irusta et al., 2015), and reduce urine protein and inhibit renal fibrosis in T2DM patients (Amador-Licona, Guizar-Mendoza, Vargas et al., 2000,Cavaglieri, Day, Feliers et al., 2015), thus playing a certain role in renal protection.

Previous studies of our research team have demonstrated the potential protective effect of metformin on the pathological process of inflammation and fibrosis in DKD (Wu, Qin, Ren et al., 2018). The antioxidant enzyme system [superoxide dismutase (SOD), catalase (CAT) and glutathione peroxidase (GSH-PX)], malondialdehyde (MDA), and hypoxia inducible factor1α (HIF1α) reflect the damage of oxidative stress (Takiyama and Haneda, 2014,Goc, Szaroma, Kapusta et al., 2017), while Beclin 1 (BECN1), autophagy related gene 12 (Atg12), microtubule-associated proteins 1A/1B light chain 3B (LC3B), and sequestosome-1 (SQSTM1/P62, p62) correlated with autophagy activity (Vucicevic, Misirkic-Marjanovic, Paunovic et al., 2014), considered to be biomarkers of oxidative stress and autophagy to assess diabetic kidney injury. In addition, metformin can inhibit oxidative stress and promote autophagy in renal cells and thereby protect renal tissues by activating the proteins adenosine monophosphate-activated protein kinase (AMPK) and silent mating type information regulation 2 homolog-1 (sirtuin-1, SIRT1) (Takiyama and Haneda, 2014,Alhaider, Korashy, Sayed-Ahmed et al., 2011,Li, Gui, Ren et al., 2016,Arunachalam, Samuel, Marei et al., 2014). Forkhead box protein O1 (FoxO1) is an important regulator involved in oxidative stress and anti-autophagy process. AMPK and SIRT1 can make synergistic actions together regulating kidney damage caused by diabetes via FoxO1-mediated oxidative stress and autophagy (Park, Lim, Kim et al., 2016,Ji, Wu, Ma et al., 2014,Wu, Zhang, Ma et al., 2012). Therefore, there may be a potential association between metformin and AMPK/SIRT1- FoxO1 mediated DKD regulation.

Our research is aimed to explore the molecular mechanism of metformin alleviating DKD via AMPK/SIRT1-FoxO1 pathway by measuring the levels of oxidative stress and autophagy related factors in diabetic rats with high-fat diet and low-dose streptozotocin (STZ) injection *in vivo* and rat mesangial cells (RMCs) cultured with high glucose *in vitro*.

2. Materials and Methods

2.1 Animal feeding

Eight weeks old male Sprague-Dawley rats (Beijing Vital River Laboratory Animal Technology Co., Ltd.) were fed in a standard specific pathogen free (SPF) laboratory with 3 rat/cage, free access to food and water, at room temperature 23 ± 2°C, humidity 55 ± 5%, 12 h light/dark cycle. All experiments were conducted daily from 9 to 11 am to avoid the effects of circadian rhythm, and were approved by the Institutional Animal Care and Use Committee (IACUC) of the First Affiliated Hospital of China Medical University (Approval no-2017112).

2.2 Cell culturing

RMCs (ATCC®CRL-2573™, purchased from American Type Culture Collection) were inoculated into 75 cm^2 culture flasks in Dulbecco's Modified Eagle Medium(D-MEM) medium (Life Technology, Carlsbad, CA, USA) with 15% fetal bovine serum (labeled as North American origin, Gibco, USA) with saturated humidity at 37 ℃ in 5% CO^2 atmosphere. Cells in their 5^{th} to 9^{th} generation of logarithmic growth phase were inoculated into 75 cm^2 culture flasks at a ratio of 4×10^6 /flask and 6-well tissue culture plates of 5×10^5 /well. RMCs were synchronized via starvation in Opti-MEM (Gibco, USA) for 24 h when cell confluency reached 70-80% and then cultured for 24 h respectively with normal glucose (NG, 5.5 mmol/L glucose), high mannitol (HM, 5.5 mmol/L glucose+24.5 mmol/L mannitol) and high glucose (HG, 30 mmol/L glucose). Cell samples were collected and stored at -196℃. The experimental flow chart is shown in Figure 1.

2.3 Diabetic modeling and intervention

We used a well-established high-fat diet and low dose streptozotocin (STZ, S0130, Sigma-Aldrich, USA) diabetic rat model (Bavenholm, Pigon, Ostenson et al., 2001,Zhang, Ye, Li et al., 2003,Srinivasan, Viswanad, Asrat et al., 2005). Rats were fed with a high-fat diet (D12492, 60 kcal% fat, 20 kcal% carbohydrate, 20 kcal% protein, with a total energy of 5.24 kcal/gm, Research Diets, Inc., USA) followed by 1-week adaptive feeding. After 2 weeks feeding, the rats fasted for 12-16 h and were injected with low dose STZ (35mg/kg, dissolved with cold 0.1 M citrate buffer pH 4.5) (Akgun and Ertel, 1985). OneTouch Ultra™ glucometer and test paper (Johnson &

Johnson, USA) of diabetic rats was measured by tail vein blood collection when the condition of diabetes was stable after 72 h of STZ injection. Rats with significant hyperglycemia (blood glucose > 16.7mmol/L) accompanied by polydipsia and polydipsia were randomly divided into 2 groups: the diabetic group with placebo treatment(DM，n = 6 rats , double distilled water used as placebo for 8 weeks) and the metformin intervention group (MET, n = 6 rats , Bristol-Myers Squibb Company, USA, 250 mg/kg/d intragastrically administered for 8 weeks) (A.K. Madiraju, Y. Qiu, R.J. Perry et al., 2018, D.K. DePeralta, L. Wei, S. Ghoshal et al., 2016, Zhai, Gu, Yang et al., 2015). Over the course of the study, both groups were given a long-term, high-fat diet. Meanwhile, a control diet (D12450J, 10 kcal% fat, 20 kcal% carbohydrate, 20 kcal% protein, with a total energy of 3.85 kcal/gm, Research Diets, Inc., USA) was used to feed rats in the same age as the normal control group (NC, n= 6 rats) (Pellizzon and Ricci, 2018). The experimental flow chart is shown in Figure 1 as well.

2.4 Gene silencing and drug treatment

RMCs were inoculated into 6-well culture plates (962 mm^2) and then transfected with FoxO1, AMPK, SIRT1 and normal control small interfering RNA (siRNA) for gene silencing via Lipofectamine 2000 (Invitrogen, USA) after 24 h synchronization of Opti-MEM starvation. They were transfected respectively with FoxO1 or the normal control siRNA 100 pmol / 4 μg for 24 h (si- FoxO1 or si-NC), AMPK, SIRT1 or the normal control siRNA 10 μmol/L for 6 h (si-SIRT1, si-AMPK or si-NC, sc-108043, sc-270142 and sc-37007, Santa Cruz Biotechnology, USA). The siRNA sequences designed and synthesized by GenePharma (Shanghai, China) were as follows: 5'- CCA GGC ACC UCA UAA CAA ATT - 3' for siRNA-rat-FoxO1 Forward, 5'- UUU GUU AUG AGG UGC CUG GTT - 3' for siRNA-rat-FoxO1 Reverse; 5'- UUG UCC GAA CGU GUC ACG UTT - 3' for siRNA-rat-negative control Forward, 5'- ACG UGA CAC GUU CGG AGA ATT - 3' for siRNA-rat-negative control Reverse. In addition, metformin (10, 50 and 100 μmol/L, 1115-70-4, Sigma-Aldrich, USA) was used to pretreat RMCs for 1 h (MET 10, MET 50 and MET 100) according to the methods in our previous studies (Wu et al., 2018,Shao, Lv, Wu et al., 2016). Then these RMCs were collected after 24 h normal or high glucose culturing and stored in liquid nitrogen for the follow-up experiment.

2.5 Collection of biochemical indicators

After 8 weeks treatment, rats of all groups were kept individually in metabolic cages for 24 h after adaptation to measure food, water intake and 24 h-urine volume (24h-uVol) and collect urinary samples (Wu, Zhang, Liu et al., 2015). Meanwhile, non-invasive blood pressure analysis of rats was measured using the BP-2010 Series Blood Pressure Meter (Softron Biotechnology, Beijing, China) with the latest implementation of the caudal artery method (Zhao, Kong, Li et al., 2014). Rats were measured for systolic blood pressure (SBP) and diastolic blood pressure (DBP), and each rat was measured 3 times to obtain average blood pressure value. Intraperitoneal glucose tolerance test (IPGTT) and insulin release test (IRT) were performed: Rats fasted for 12 h, and glucose (2 g/kg) was administered intra-peritoneal injection (Yuan, Wang, Lu et al., 2013). Blood samples were collected from periorbital venous plexuses at 6 time points including 0, 5, 10, 30, 60 and 120 min, respectively. Both serum and plasma (with anti-coagulant) samples collected were stored at -80°C for further use.

2.6 Renal histology

At the end of experiment, rats were anesthetized by isoflurane (1.38-2.4 % for induction and 2.0-3.0 % for maintenance, RWD Life Science Co., Ltd, Shenzhen, China) after measurement of body weight (BW). Blood samples were collected via cardiac puncture (Hoff, 2010). Renal tissues were perfused with cold phosphate buffer saline (PBS) buffer until effluent was clear of blood, then renal capsules were repeatedly perforated with a 23G needle (20), and the kidney samples were immersed in freshly 4% paraformaldehyde (Mitrou, Morrison, Mousavi et al., 2015). The kidney and white adipose weight (KW and WAW) were measured and the kidney and body fat ratio (KR and BFR) were calculated as follows: KR =KW(g)/ BW(g)×100%, BFR=WAW (g) /BW (g) ×100%]. The right kidney tissues were stored at -196℃ liquid nitrogen for further analysis, while the left kidney tissues were perfused at 100 mmHg with 4% paraformaldehyde (Sigma, USA) for fixation at 4°C overnight. Formalin fixed renal tissues were trimmed longitudinally and processed for histology. Paraffin embedded tissue blocks were sectioned at 5 μm thickness with a Rotary Microtome. Kidney sections were stained with Hematoxylin & Eosin (HE) stain,

Periodic Acid-Schiff (PAS) stain and Masson stain. The stained slides were examined under microscope at 400 times magnification.

Six sections were randomly selected in each group, and were analyzed using Image-Pro Plus 6.0 software (Media Cybernetics, Silver Spring, MD, USA). The glomerular volumes were calculated as $Area^{1.5} \times 1.38/1.01$ (I. Vaněčková, P. Kujal, Z. Husková et al., 2012). The mesangial expansion index (MEI) was scored at four levels as described previously (W.A. Border, S. Okuda, L.R. Languino et al., 1990, X.Q. Li, W. Tian, X.X. Liu et al., 2016), the MEI scores are defined as follows: 0, normal glomeruli; 1, matrix expansion occurring in up to 50% of glomeruli; 2, matrix expansion occurring in 50–75%; 3, matrix expansion occurring in 75–100%. Fibrosis levels were expressed as the ratio of stained blue fibrotic tissues and total measured area using Image-Pro Plus 6.0 software (X.Q. Li, W. Tian, X.X. Liu et al., 2016).

2.7 Fluorescence immune-double localization

Renal tissue samples were incubated with primary antibody, rabbit anti-rat SIRT1 and rabbit anti-rat FoxO1 (1:400 and 1:100, #9475 and #2880, Cell Signaling Technology, USA), at 4℃ overnight, then shaked with two different second antibody, Alexa Fluor® 488 Conjugate anti-rabbit IgG and Alexa Fluor® 555 Conjugate anti-rabbit IgG (1:1000, #4412 and #4413, Cell Signaling Technology, USA), at room temperature for 1 h. ProLong® Gold Antifade Reagent with DAPI (#8961, Cell Signaling Technology, USA) was used for nuclear staining. The prepared slides were examined and quantified under fluorescence microscope (ECLIPSE C1, NIKON, Japan) at 400 times magnification.

2.8 Real-time PCR

Total RNA of kidney tissues and RMCs was extracted using Trizol RNA isolating regents (TaKaRa Biotechnology, Japan). 1 μg total RNA was reverse-transcribed into cDNA based on the manual of PrimerScript ® RT reagent Kits with gDNA Eraser (Perfect Real Time) Kits (TaKaRa Biotechnology, Japan). Real-time PCR was performed by SYBR® Premix ExTaq™ II kits (TaKaRa Biotechnology, Japan) and RNA primers as follows: SIRT1-F: 5' - TAC CAG AAC AGT TTC ATA GAG CCA T - 3', SIRT1-R: 5' - CAA AAT GTA GAT GAG GCA GAG GTT- 3'; FoxO1-F: 5' - TCG AAC CAG CTC AAA CGC - 3', FoxO1-R: 5' -

GGT GGA TAC ACC AGG GAA TG - 3'; AMPK-F: 5' - GCT CGC AGT GGC TTA TCA T - 3', AMPK-R: 5' - TGG ACA GCG TGC TTT GG - 3'; β-actin-F: 5' - TGA CAG GAT GCA GAA GGA GAT TAC - 3', β-actin-R: 5' - GAG CCA CCA ATC CAC ACA GA - 3'. The total reaction volume was 20 μl with 2 μl cDNA in a template. PCR amplification conditions were as follows: initial denaturation at 95□ for 3 min, followed by denaturation 40 cycles at 95□ for 12 s, annealing at 62□ for 30 s, and extension at 72□ for 30 s. TaKaRa Thermal CyclerDice® Real Time System was used to detect the fluorescence and the same experimental conditions were repeated three times. The threshold cycle was measured using the 2 ^ (- Δ Δ Ct) method in reference to β-actin.

2.9 Western blotting

Whole kidney tissues and RMCs were lysed in RIPA lysis buffer with phenylmethanesulfonylfluoride (PMSF) protease inhibitor. The total protein content was analyzed by Pierce™ BCA protein assay kit (Thermo Fisher Scientific, USA) based on a standard control of bovine serum albumin (BSA). Samples added with 5× loading buffer were boiled at 100 °C for 10 min. Equivalent protein samples (40 μg / tissue sample and 50 μg / cell sample) were separated respectively with 10% sodium dodecyl sulfate-polyacrylamide gel electrophoresis (SDS-PAGE), then transferred to polyvinylidene fluoride (PVDF) membranes (0.45 μm, Millipore, USA). LC3B was transferred for 30 min; AMPKα, pAMPKα, Atg12, BECN1, p62 and β-actin for 1 h, while SIRT1, FoxO1, p FoxO1 and HIF1α for 2 h. Membranes were blocked in tris buffered saline +Tween 20 (TBS-T) with 5 % BSA at room temperature for 2 h, then incubated with primary antibodies of the appropriate content (in Table 1) at 4℃ overnight. After extensive washing, membranes were incubated with secondary antibodies of the appropriate content (in Table 1) and then reacted with Pierce™ ECL Plus Substrate (Thermo Fisher Scientific, USA). MicroChemi 4.2 bioimaging system (Jerusalem, Israel) was used to measure immunoreactive bands, which were repeated three times under the same experimental conditions.

2.10 CLIA and ELISA

Chemiluminescent immunoassay (CLIA) were adopted to observe the levels of total cholesterol (TC), triglycerides (TG), low density lipoprotein Cholesterol

(LDL-C), high density lipoprotein Cholesterol (HDL-C), creatinine (Cr) and blood urea nitrogen (BUN)(A111-1, A110-1, A113-1, A112-1, C011-2 and C013-1, Nanjing Jiancheng Bioengineer Institute, China), while enzyme linked immunosorbent assays (ELISAs) were used to measure the levels of insulin (INS, CEA448Ra, USCN, USA), hemoglobin A1c (HbA1c, CEA190Ra, USCN, USA), and albumin levels (MAU, CSB-E12991r, CUSABIO, USA).

Fasting blood glucose (FPG) and fasting insulin (FINS) were collected by intraperitoneal glucose tolerance test (IPGTT) and insulin release test (IRT). Homeostatic model of insulin resistance index (HOMA-IR) and insulin sensitivity index (ISI) were used to evaluate the insulin resistance and sensitivity (Wang, Jin and Sun, 2018) using the formula: HOMA-IR=FPG (mmol/L) ×FINS (mIU/L)/22.5, and ISI=-ln [FPG (mmol/L) ×FINS (mIU/L)]. Graphpad Prism 8.0 software was used to measure the area under curve of glucose (AUC GLU), the area under curve of insulin (AUC INS) and the area under curve glucose/insulin ratios (AUC ratio), while the urinary albumin creatinine ratios (UACR) were used to evaluate the urinary protein (Yu, Yang, Tian et al., 2015).

SOD, GSH-PX, CAT and MDA detection kits (A001-3, A007-1-1, A005, A003-1, Nanjing Jiancheng Bioengineer Institute, China) were used for the measurement of antioxidants and oxidative stress in rat renal tissue lysates, rat serum and cell supernatant by a full wavelength microarray (BioTek Power Wave XS) with the absorbance at 450nm, 405nm, 412nm and 523nm wavelength. Three wells were set for each sample, and the concentration was calculated based on the standard curve.

2.11 Cell Counting Kit-8

Cell suspension was prepared after trypsin digestion and cell density was adjusted at the ratio of 5×10^3/100 μl/well in a 96-well plate. RMCs were cultured respectively with normal and high glucose for 24, 48 and 72 h with saturated humidity at 37℃ in 5% CO^2. Each well was added with 10 μl detection solution and sequentially incubated for 2 h according to the manufacturer instructions of Cell Counting Kit-8 (CCK-8, Dojindo, Japan). The absorbance at 450 nm wavelength was measured by a full wavelength microarray (BioTek Power Wave XS) with three wells for each sample.

2.12 Statistical analysis

IBM SPSS Statistics Version 25.0 and GraphPad Prism 8.0 software were used to analyze the data. After Kolmogorov-Smirnov normality test with Dallal-Wilkinson-Lillie for *P* value, data were expressed as mean ± standard deviation (mean±SD). Differences between three or more groups were analyzed by one-way ANOVA followed by Bonferroni test as a multiple-comparison test. $P < 0.05$ was considered of statistical significance.

3. Results

3.1 The levels of biochemical indicators in metformin treated diabetic rats

Compared with the NC group, BW, BFR and HDL-C were significantly decreased in the DM group, but these indicators were elevated in the MET group in comparison with the DM group ($P < 0.05$, Figure I and J). HbA1c, blood lipid (TG, TC, LDL-C), renal function (BUN, Cr) and urinary protein (UACR) were significantly increased in the DM group, however, reduced after metformin treatment ($P < 0.05$, Figure F, J, L, and M). Food and water intake, 24h-UV, and KR in the DM group were higher than the NC group, but left unchanged between DM and MET groups ($P > 0.05$, Figure K and H). Moreover, blood pressure (SBP and DBP) were not significantly different among the three groups ($P > 0.05$, Figure G).

The results of IPGTT and IRT showed that compared with NC group, HOMA-IR and AUC GLU were elevated in the DM group, and reduced after metformin treatment. Meanwhile, ISI, AUC INS and AUC ratio in DM group were lower than NC group, but these levels in MET group were significantly higher than DM group ($P < 0.05$, Figure 2 A-E).

3.2 Changes of diabetic renal tissues induced by metformin

To assess the effect of metformin on diabetic rats, we performed histochemical staining to analyze and quantify the pathological changes of renal tissues. The results showed that compared with the NC group, the glomerular vascular network was severely damaged with the loss of normal reticular structure and typical pink hyaline degeneration appeared in the DM group. The burgundy stain of glycogen and the blue stain of fibrous tissues were markedly deepened as well. The MET group also lost its normal structure, but the lesion was generally less severe than that of the DM group (Figure 3A-C). The glomerular volume, mesangial expansion, assessed by MEI, and fibrosis level in the DM group was significantly larger than that of NC group but inhibited in the MET group ($P < 0.05$, Figure 3E). Quantitation of fluorescence immune-double localization showed that relative expression of FoxO1/DAPI was up-regulated, and SIRT1/DAPI was down-regulated in the DM group. However, FoxO1/DAPI was inhibited, and SIRT1/DAPI was elevated in the MET group ($P < 0.05$, Figure 3D and F).

Real-time PCR results showed that compared with the NC group, the relative expression of AMPK and SIRT1 mRNA were significantly decreased, while FoxO1

increased in the kidney tissues of the DM group. Compared with the DM group, AMPK and SIRT1 mRNA up-regulated, while FoxO1 down-regulated in the MET group ($P < 0.05$, Figure 4C). Protein expression of pAMPKα/AMPKα, SIRT1, BECN1, Atg12, and LC3B reduced significantly, but pFoxO1/FoxO1, HIF1α, and p62 were elevated in the DM group in western blot analysis. In the MET group, pAMPKα/AMPKα, SIRT1, BECN1, Atg12, and LC3B were elevated, while pFoxO1/FoxO1, HIF1α, and p62 were reduced ($P < 0.05$, Figure 4A and B). The expression levels of SOD, CAT and GSH-PX in renal tissues of the DM group were significantly higher than those of the NC group, while MDA were significantly lower. SOD, CAT, and GSH-PX levels in the MET group were higher than those of the DM group, while MDA was significantly lower. ($P < 0.05$, Figure 4D).

3.3 Changes of related factors in high-glucose cultured RMCs

To explore the effect of high glucose on RMCs, cells were cultured respectively with normal glucose, mannitol and high glucose (NG, HM and HG). Results as shown in Figure 5, compared with the NG group, the relative expression of AMPK and SIRT1 mRNA in the HG group were significantly decreased, while FoxO1 were increased. Protein levels of pAMPKα/AMPKα, SIRT1, BECN1, Atg12 and LC3B were significantly down-regulated, but pFoxO1/FoxO1, HIF1α and p62 were up-regulated in the HG group. The levels of SOD, CAT and GSH-PX in cell supernatant were significantly reduced, MDA was increased, and OD values at 450 nm wavelength of CCK-8 were significantly increased ($P < 0.05$). However, there was no statistical difference in these parameters between HM and NG groups ($P > 0.05$), thus excluding the influence of osmotic pressure on RMCs.

3.4 Proliferation changes of metformin with different concentrations in RMCs

CCK-8 was used to detect the proliferation of RMCs on intervention of different concentrations of metformin (NG, NG+10, NG+50 and NG+100). The results showed that compared with the NG group, the OD 450 nm in the NG+10, NG+50 and NG+100 group were significantly reduced ($P < 0.05$, Figure 6A), and the OD 450 nm in the NG+50 group was the wave trough. Therefore, the concentration of 50 μmol/L metformin was selected as the normal and high glucose metformin intervention group (NG+MET and HG+MET) for follow-up experiments.

3.5 Expression of related factors in high-glucose cultured RMCs with metformin treatment

To determine the effect of metformin, the appropriate metformin concentration (50 μmol/L) was adopted to pre-treat RMCs into normal glucose, normal glucose metformin intervention, high glucose and high glucose metformin intervention group (NG, NG+MET, HG and HG+MET). The results showed that compared with the NG group, the relative expression of AMPK and SIRT1 mRNA in the NG+MET group significantly decreased, while FoxO1 mRNA increased. The relative expression of pAMPKα/AMPKα, SIRT1, BECN1, Atg12 and LC3B were significantly elevated, while pFoxO1/FoxO1, HIF1α and p62 were significantly reduced. The levels of SOD, CAT and GSH-PX in cell supernatant were significantly increased, while MDA decreased. OD 450 nm of CCK-8 was significantly decreased in the NG+MET group. The HG+MET group showed the same changes compare with the HG group. The relative expression of AMPK and SIRT1 mRNA in the HG+MET group decreased, while FoxO1 mRNA increased compared with the HG group. The protein levels of pAMPKα/AMPKα, SIRT1, BECN1, Atg12, and LC3B were reduced, while pFoxO1/FoxO1, HIF1α, and p62 were elevated. The levels of SOD, CAT, and GSH-PX in the HG+MET group were lower, while MDA was higher than the HG group. OD values were significantly decreased in the HG+MET group. ($P < 0.05$, Figure 6 B-F).

3.6 Expression of related factors in high-glucose cultured RMCs with AMPK, SIRT1 and FoxO1 gene silencing

To clarify the upstream and downstream relationship of AMPK, SIRT1 and FoxO1 in RMCs, cells were divided into high-glucose, high-glucose siRNA normal control, high-glucose AMPK, SIRT1 and FoxO1 siRNA transfected groups (HG, HG+ si-NC, HG+ HG+si-AMPK, HG+si-SIRT1 and HG+si-FoxO1). Real-time PCR and western blot results showed that the relative expression of pAMPK /AMPK and SIRT1 in the HG+si-AMPK and HG+si-SIRT1 groups were significantly lower, and pFoxO1/FoxO1 were higher than those in the HG group. Compared with the HG group, the relative expression of pFoxO1/FoxO1 in the HG+si-FoxO1 group was significantly decreased ($P < 0.05$), but there were no significant changes in pAMPK /AMPK and SIRT1 levels ($P > 0.05$). OD values increased in HG+si-AMPK and HG+si-SIRT1 groups, but decreased in the HG+si-FoxO1 group ($P < 0.05$). In

addition, there were no statistically significant differences of mRNA and protein expression between HG and HG+ si-NC groups ($P > 0.05$, Figure 7), excluding the effect of transfection on RMCs.

4. Discussion

T2DM is a metabolic disease, whose main pathological features are hyperglycemia and insulin resistance accompanied with typical clinical characteristics, polydipsia, polyphagia and polyuria (Marathe, Gao and Close, 2017,Kalsi, Chopra and Sood, 2015), which contributes to diabetic microvascular complications, DKD (with incidence of 20–40% in diabetes) (Stratton, Adler, Neil et al., 2000). The clinical manifestation of DKD is characterized by progressive and slow development of proteinuria with pathological features of thickening of the glomerular basement membrane, mesangial hyperplasia, glomerular hypertrophy and deposition of excess extracellular matrix (Ziyadeh, 1993,Afkarian, Zelnick, Hall et al., 2016), leading to end stage renal disease (ESRD) (Saran, Robinson, Abbott et al., 2018).

Metformin can improve insulin resistance and glucose tolerance and interfere with insulin resistance, glycolipid, fatty acid and liver metabolism (De Jager et al., 2005,Naderpoor, Shorakae, De et al., 2015), and it is beneficial for numerous diseases with independent risk factors of these metabolism process (Di et al., 2015,Fruci, Giuliano, Mazza et al., 2013,Goldberg, Aroda, Bluemke et al., 2017) especially associated with complications of T2DM like diabetic retinopathy, neuropathy, as well as nephropathy (Alhaider et al., 2011,Li, Ryu, Munie et al., 2018,Ma, Yu, Liu et al., 2015, Aschenbrenner, 2016). In the present study, we explored whether metformin attenuates inflammatory and fibrosis factors in RMCs following high glucose induced stress (Wu et al., 2018).

A well-established T2DM rat model with high-fat diet feeding for 2 weeks to induce insulin resistance symptoms and low dose intraperitoneal injection of STZ to partly destroy the function of pancreatic β cells (Bavenholm et al., 2001,Zhang et al., 2003,Srinivasan et al., 2005), and a high glucose induced RMCs model were established in our present research to study the metformin treatment of DKD. We can observe hyperglycemia and insulin resistance, typical ‘three polys and one loss’ diabetic symptoms (polydipsia, polyphagia, polyuria and weight loss) and disorders of blood lipids in diabetic rats. Urinary protein and renal ratio increased, glomerular structure destroyed with obvious hyaline degeneration accompanied with glycogen redness and collagenous fibrosis blue stain. However, there is no changes in blood pressure were discovered in diabetes groups. These findings indicated the successful modeling of T2DM rats and diabetic kidney functional insufficiency. Moreover, there was abnormal proliferation in RMCs cultured with high glucose *in vitro*. Metformin

was demonstrated to reduce insulin resistance, maintain blood glucose stability, relieve dyslipidemia and body fat, attenuate kidney dysfunctions and proteinuria, and alleviate diabetes renal damage. Moreover, glycogen redness and collagen blueness reduced, and abnormal proliferation alleviated in high glucose+metformin incubation, indicating that renal structural damage was relieved by metformin treatment. Therefore, the above studies have shown that metformin can alleviate disorders of glycolipid metabolism, renal damage and proteinuria in both diabetic rats and RMCs.

The two important mechanisms of renal injury in DKD are oxidative stress and impaired autophagy (Takiyama and Haneda, 2014,Li et al., 2016). The antioxidant enzyme system (SOD, CAT and GSH-PX) indicates the ability of scavenging reactive oxygen species, while HIF1α and the end product of lipid peroxidation MDA reflects the damage of oxidative stress (Takiyama and Haneda, 2014,Goc, Szaroma, Kapusta et al., 2017). In the advanced stage of diabetes, derangements in intracellular environment greatly inhibit renal autophagy, which eventually leads to autophagy decompensation and accelerates the progression of DKD (Yang, Livingston, Liu et al., 2018). BECN1 is an important factor in the initiation of autophagy. Atg gene controls the formation of autophagosome through Atg12-Atg5 and LC3B complex. LC3B makes action in the whole process of autophagy, the two of which reflect the levels of autophagy. Autophagy receptor protein p62 is a degradation product of late autophagy and negatively correlated with autophagy activity (Vucicevic, Misirkic-Marjanovic, Paunovic et al., 2014). The aforementioned biomarkers can be used as markers of oxidative stress and autophagy to assess diabetic kidney injury. We found that protein expression of BECN1, Atg12 and LC3B were decreased in diabetic rat kidneys, while HIF1α and p62 were increased. The levels of SOD, CAT and GSH-PX in rat serum and renal tissues reduced, while MDA was elevated. The same phenomenon was observed in high glucose cultured RMCs. This suggests that DKD may affect the physiological processes in renal tissues and RMCs by enhancing oxidative stress and weakening autophagy.

The transcription factor family, FoxO, plays a central role in cell proliferation and survival by regulating cell cycle arrest, DNA repair and apoptosis in endothelial cells (Papanicolaou, Izumiya and Walsh, 2008). Among them, FoxO1 is considered as an important regulatory factor involved in oxidative stress, apoptosis promotion and autophagy inhibition in diabetic animal models. Resveratrol can reduce the phosphorylation of downstream effecting factors FoxO1 and FoxO3a via the

phosphorylation of SIRT1 and AMPK, thereby alleviate the oxidative stress and cell apoptosis, reduce the accumulation of extracellular matrix and decrease glomerular lesions in the renal tissues of high-glucose-mediated T2DM db/db mice (Park et al., 2016,Ji et al., 2014,Wu et al., 2012). Besides, AMPK and SIRT1, as nutrient sensory signals, also play a regulatory role in autophagy of DKD (Kume, Koya, Uzu et al., 2014). Nutrient deprivation or low energy can enhance autophagy by activating AMPK and SIRT1 under normal conditions, while hyperglycemia inhibits the activity of AMPK and SIRT1 and inhibits autophagy under the condition of diabetes (Yang et al., 2018,Kitada, Ogura, Monno et al., 2017). Therefore, AMPK/SIRT1-FoxO1 pathway may be a potential pathological link in diabetic kidney injury.

Previous studies have found that metformin can inhibit the process of oxidative stress, promote autophagy induction, and protect acute kidney injury by activating AMPK (Takiyama and Haneda, 2014,Alhaider et al., 2011,Li et al., 2016). Other studies suggest that metformin inhibit the growth of estrogen-dependent endometrial cancer cells by activating the AMPK-FoxO1 signaling pathway (Zou, Hong, Luo et al., 2016) Moreover, it can negatively regulate FoxO1-dependent cell cycle arrest and apoptosis gene transcription by activating SIRT1, and protect endothelial cells from hyperglycemia-induced senescence and apoptosis (Arunachalam et al., 2014). These studies suggests that metformin protects against on diabetic renal injury through AMPK/SIRT1-FoxO1 pathway, and may regulate the oxidative stress and autophagy.

To explore the pathological mechanism of DKD, we established a model of T2DM in rats with high fat diet and STZ *in vivo* and high glucose cultured RMCs *in vitro*, and utilized gene silencing technology to transfect AMPK, SIRT1 and FoxO1 siRNA into RMCs. The results showed that the protein levels of pAMPKα and SIRT1 were up-regulated and pFoxO1 was down-regulated in both RMCs and diabetic rats. Antioxidant enzymes (SOD, CAT, GSH-PX) decreased, while HIF1α and MDA increased. Autophagy related markers BECN1, Atg12 and LC3B were reduced, while p62 was elevated. Gene silencing of AMPK and SIRT1 can enhance activity to each other and up-regulate pFoxO1, but FoxO1 siRNA cannot change the expression of pAMPK and SIRT1. These results suggested that AMPK/SIRT1-FoxO1 pathway may participate in the regulation of oxidative stress and autophagy in DKD.

We established the intervention of metformin in diabetic rats and high glucose cultured RMCs to study the possible regulatory mechanism. The results showed that metformin up-regulated pAMPK, SIRT1, HIF1α, MDA, BECN1, Atg12 and LC3B,

and down-regulated pFoxO1, antioxidant enzyme and p62 in both rats and RMCs. It suggests that metformin can alleviate oxidative stress and inhibit autophagy in renal lesions by activating AMPK and SIRT1 and inhibiting FoxO1.

In conclusion, we found that metformin can significantly alleviate the abnormal glucose and lipid metabolism and renal damages in T2DM rats. Metformin can improve the oxidative stress and inhibit autophagy of RMCs by regulating AMPK/SIRT1-FoxO1 pathways, thereby alleviating the development process of DKD. The possible molecular mechanisms are shown in Figure 8.

Acknowledgments

Our team would like to thank the Laboratory Medicine, Nephrology Laboratory, Central Laboratory and the Laboratory of Endocrine and Metabolism of the First Hospital of China Medical University for technical assistance and equipment support. This study was supported by the Higher School "High-end Talent Team Construction" of Liaoning Province (Grant number: [2014]187), and the "Natural Science Foundation of Liaoning Province (Grant number: 201602862)", Liaoning Province, P.R., China.

Conflicts of Interest

The authors declare that they have no conflicts of interest.

Ethical use of Animals

All animals were kept in a pathogen-free environment and fed ad lab. The procedures for care and use of animals were approved by the Institutional Animal Care and Use Committee (IACUC) of the First Affiliated Hospital of China Medical University (Approval no-2017112), and all experimental operations were complied with Guide for Laboratory Animal Care and Use and Animal Welfare Act. All applicable institutional and governmental regulations concerning the ethical use of animals were followed.

References

[1] Saran, R., Robinson, B., Abbott, K.C., Agodoa, L.Y.C., Bragg-Gresham, J., Balkrishnan, R., Xue, D., Eckard, A., Eggers, P.W. and Gaipov, A., 2018. US Renal Data System 2017 Annual Data Report: Epidemiology of Kidney Disease in the United States, American Journal of Kidney Diseases. 71, A7.

[2] 2015. Standards of medical care in diabetes--2015: summary of revisions, Diabetes Care. 38 Suppl, S4.

[3] American Diabetes, A., 2018. 8. Pharmacologic Approaches to Glycemic Treatment: Standards of Medical Care in Diabetes-2018, Diabetes Care. 41, S73-S85.

[4] De Jager, J., Kooy, A., Lehert, P., Bets, D., Wulffelé, M.G., Teerlink, T., Scheffer, P.G., Schalkwijk, C.G., Donker, A.J. and Stehouwer, C.D., 2005. Effects of short-term treatment with metformin on markers of endothelial function and inflammatory activity in type 2 diabetes mellitus: a randomized, placebo-controlled trial, J. Intern. Med. 257, 100-9.

[5] Di, P.M., Parborell, F., Irusta, G., Pascuali, N., Bas, D., Bianchi, M.S., Tesone, M. and Abramovich, D., 2015. Metformin regulates ovarian angiogenesis and follicular development in a female polycystic ovary syndrome rat model, Endocrinology. 156, 1453-63.

[6] Amador-Licona, N., Guizar-Mendoza, J., Vargas, E., Sanchez-Camargo, G. and Zamora-Mata, L., 2000. The short-term effect of a switch from glibenclamide to metformin on blood pressure and microalbuminuria in patients with type 2 diabetes mellitus, Arch Med Res. 31, 571-5.

[7] Cavaglieri, R.C., Day, R.T., Feliers, D. and Abboud, H.E., 2015. Metformin prevents renal interstitial fibrosis in mice with unilateral ureteral obstruction, Mol Cell Endocrinol. 412, 116-22.

[8] Wu, C., Qin, N., Ren, H., Yang, M., Liu, S. and Wang, Q., 2018. Metformin Regulating miR-34a Pathway to Inhibit Egr1 in Rat Mesangial Cells Cultured with High Glucose, Int J Endocrinol. 2018, 6462793.

[9] Takiyama, Y. and Haneda, M., 2014. Hypoxia in diabetic kidneys, Biomed Res Int. 2014, 837421.

[10] Goc, Z., Szaroma, W., Kapusta, E. and Dziubek, K., 2017. Protective effects of melatonin on the activity of SOD, CAT, GSH-Px and GSH content in organs of mice after administration of SNP, Chin J Physiol. 60, 1-10.

[11] Vucicevic, L., Misirkic-Marjanovic, M., Paunovic, V., Kravic-Stevovic, T., Martinovic, T., Ciric, D., Maric, N., Petricevic, S., Harhaji-Trajkovic, L., Bumbasirevic, V. and Trajkovic, V., 2014. Autophagy inhibition uncovers the neurotoxic action of the antipsychotic drug olanzapine, Autophagy. 10, 2362-78.

[12] Alhaider, A.A., Korashy, H.M., Sayed-Ahmed, M.M., Mobark, M., Kfoury, H. and Mansour, M.A., 2011. Metformin attenuates streptozotocin-induced diabetic nephropathy in rats through modulation of oxidative stress genes expression, Chem Biol Interact. 192, 233-42.

[13] Li, J., Gui, Y., Ren, J., Liu, X., Feng, Y., Zeng, Z., He, W., Yang, J. and Dai, C., 2016. Metformin Protects Against Cisplatin-Induced Tubular Cell Apoptosis and

Acute Kidney Injury via AMPKalpha-regulated Autophagy Induction, Sci Rep. 6, 23975.

[14] Arunachalam, G., Samuel, S.M., Marei, I., Ding, H. and Triggle, C.R., 2014. Metformin modulates hyperglycaemia-induced endothelial senescence and apoptosis through SIRT1, Br. J. Pharmacol. 171, 523-35.

[15] Park, H.S., Lim, J.H., Kim, M.Y., Kim, Y., Hong, Y.A., Choi, S.R., Chung, S., Kim, H.W., Choi, B.S., Kim, Y.S., Chang, Y.S. and Park, C.W., 2016. Resveratrol increases AdipoR1 and AdipoR2 expression in type 2 diabetic nephropathy, J Transl Med. 14, 176.

[16] Ji, H., Wu, L., Ma, X., Ma, X. and Qin, G., 2014. The effect of resveratrol on the expression of AdipoR1 in kidneys of diabetic nephropathy, Mol. Biol. Rep. 41, 2151-9.

[17] Wu, L., Zhang, Y., Ma, X., Zhang, N. and Qin, G., 2012. The effect of resveratrol on FoxO1 expression in kidneys of diabetic nephropathy rats, Mol. Biol. Rep. 39, 9085-93.

[18] Bavenholm, P.N., Pigon, J., Ostenson, C.G. and Efendic, S., 2001. Insulin sensitivity of suppression of endogenous glucose production is the single most important determinant of glucose tolerance, Diabetes. 50, 1449-54.

[19] Zhang, F., Ye, C., Li, G., Ding, W., Zhou, W., Zhu, H., Chen, G., Luo, T., Guang, M., Liu, Y., Zhang, D., Zheng, S., Yang, J., Gu, Y., Xie, X. and Luo, M., 2003. The rat model of type 2 diabetic mellitus and its glycometabolism characters, Exp Anim. 52, 401-7.

[20] Srinivasan, K., Viswanad, B., Asrat, L., Kaul, C.L. and Ramarao, P., 2005. Combination of high-fat diet-fed and low-dose streptozotocin-treated rat: a model for type 2 diabetes and pharmacological screening, Pharmacol Res. 52, 313-20.

[21] Akgun, S. and Ertel, N.H., 1985. The effects of sucrose, fructose, and high-fructose corn syrup meals on plasma glucose and insulin in non-insulin-dependent diabetic subjects, Diabetes Care. 8, 279-83.

[22] Zhai, L., Gu, J., Yang, D., Wang, W. and Ye, S., 2015. Metformin Ameliorates Podocyte Damage by Restoring Renal Tissue Podocalyxin Expression in Type 2 Diabetic Rats, J Diabetes Res. 2015, 231825.

[23] Madiraju AK, Qiu Y, Perry RJ, Rahimi Y, Zhang XM, Zhang D, Camporez JG, Cline GW, Butrico GM, Kemp BE, Casals G, Steinberg GR, Vatner DF, Petersen KF and Shulman GI (2018) Metformin inhibits gluconeogenesis via a redox-dependent mechanism in vivo. Nat. Med. 24:1384-1394. doi: 10.1038/s41591-018-0125-4

[24] DePeralta DK, Wei L, Ghoshal S, Schmidt B, Lauwers GY, Lanuti M, Chung RT, Tanabe KK and Fuchs BC (2016) Metformin prevents hepatocellular carcinoma development by suppressing hepatic progenitor cell activation in a rat model of cirrhosis. Cancer 122:1216-27. doi: 10.1002/cncr.29912

[25] Pellizzon, M.A. and Ricci, M.R., 2018. The common use of improper control diets in diet-induced metabolic disease research confounds data interpretation: the fiber factor, Nutr Metab (Lond). 15, 3.

[26] Shao, Y., Lv, C., Wu, C., Zhou, Y. and Wang, Q., 2016. Mir-217 promotes

inflammation and fibrosis in high glucose cultured rat glomerular mesangial cells via Sirt1/HIF-1alpha signaling pathway, Diabetes Metab Res Rev. 32, 534-43.

[27] Wu, W., Zhang, M., Liu, Q., Xue, L., Li, Y. and Ou, S., 2015. Piwil 2 gene transfection changes the autophagy status in a rat model of diabetic nephropathy, Int J Clin Exp Pathol. 8, 10734-42.

[28] Zhao, J., Kong, D.Z., Li, Q., Zhen, Y.Q., Wang, M., Zhao, Y., Wang, D.K. and Ren, L.M., 2014. (-)Doxazosin is a necessary component for the hypotensive effect of (+/-)doxazosin during long-term administration in conscious rats, Acta Pharmacol Sin. 35, 48-57.

[29] Yuan, L., Wang, Y., Lu, C. and Li, X., 2013. Angiotensin-Converting Enzyme 2 Deficiency Aggravates Glucose Intolerance via Impairment of Islet Microvascular Density in Mice with High-Fat Diet, J Diabetes Res. 2013, 405284.

[30] Hoff, J., 2010. Technique Methods of Blood Collection in the Mouse, Lab Animal. 29, 47-53.

[31] Mitrou, N., Morrison, S., Mousavi, P., Braam, B. and Cupples, W.A., 2015. Transient impairment of dynamic renal autoregulation in early diabetes mellitus in rats, Am J Physiol Regul Integr Comp Physiol. 309, R892-901.

[32] Vaněčková I, Kujal P, Husková Z, Vaňourková Z, Vernerová Z, Certíková Chábová V, Skaroupková P, Kramer HJ, Tesař V and Červenka L (2012) Effects of combined endothelin A receptor and renin-angiotensin system blockade on the course of end-organ damage in 5/6 nephrectomized Ren-2 hypertensive rats. Kidney Blood Press. Res. 35:382-92. doi: 10.1159/000336823

[33] Border WA, Okuda S, Languino LR, Sporn MB and Ruoslahti E (1990) Suppression of experimental glomerulonephritis by antiserum against transforming growth factor beta 1. Nature 346:371-4. doi: 10.1038/346371a0

[34] Li XQ, Tian W, Liu XX, Zhang K, Huo JC, Liu WJ, Li P, Xiao X, Zhao MG and Cao W (2016) Corosolic acid inhibits the proliferation of glomerular mesangial cells and protects against diabetic renal damage. Sci Rep 6:26854. doi: 10.1038/srep26854

[35] Wang, G.H., Jin, J. and Sun, L.Z., 2018. Effect of lipoprotein-associated phospholipase A2 inhibitor on insulin resistance in streptozotocin-induced diabetic pregnant rats, Endocr J.

[36] Yu, R., Yang, Y., Tian, Y., Zhang, Y., Lyu, G., Zhu, J., Xiao, L. and Zhu, J., 2015. The mechanism played by 1,25-dihydroxyvitamin D3 in treating renal fibrosis in diabetic nephropathy, Chin.j.end.met.

[37] Marathe, P.H., Gao, H.X. and Close, K.L., 2017. American Diabetes Association Standards of Medical Care in Diabetes 2017, J Diabetes. 9, 320-324.

[38] Kalsi, D.S., Chopra, J. and Sood, A.J.I.J.o.D., 2015. Association of lipid profile test values, type-2 diabetes mellitus, and periodontitis. 6, 81.

[39] Stratton, I.M., Adler, A.I., Neil, H.A.W., Matthews, D.R., Manley, S.E., Cull, C.A., Hadden, D., Turner, R.C. and Holman, R.R.J.B., 2000. Association of glycaemia with macrovascular and microvascular complications of type 2 diabetes (UKPDS 35): prospective observational study. 321, 405.

[40] Ziyadeh, F.N., 1993. The extracellular matrix in diabetic nephropathy, Am J Kidney Dis. 22, 736-44.

[41] Afkarian, M., Zelnick, L.R., Hall, Y.N., Heagerty, P.J., Tuttle, K., Weiss, N.S. and de Boer, I.H., 2016. Clinical Manifestations of Kidney Disease Among US Adults With Diabetes, 1988-2014, Jama. 316, 602-10.

[42] Naderpoor, N., Shorakae, S., De, C.B., Misso, M.L., Moran, L.J. and Teede, H.J., 2015. Metformin and lifestyle modification in polycystic ovary syndrome: systematic review and meta-analysis, Human Reproduction Update. 21, 560-574.

[43] Fruci, B., Giuliano, S., Mazza, A., Malaguarnera, R. and Belfiore, A., 2013. Nonalcoholic Fatty Liver: A Possible New Target for Type 2 Diabetes Prevention and Treatment, International Journal of Molecular Sciences. 14, 22933-22966.

[44] Goldberg, R.B., Aroda, V.R., Bluemke, D.A., Barrettconnor, E., Budoff, M.J., Crandall, J.P., Dabelea, D., Horton, E.S., Mather, K.J. and Orchard, T.J., 2017. Effect of Long-term Metformin and Lifestyle in the Diabetes Prevention Program and its Outcome Study on Coronary Artery Calcium, Circulation. 136, 52.

[45] Li, Y., Ryu, C., Munie, M., Noorulla, S., Rana, S., Edwards, P., Gao, H. and Qiao, X., 2018. Association of Metformin Treatment with Reduced Severity of Diabetic Retinopathy in Type 2 Diabetic Patients, J Diabetes Res. 2018, 2801450.

[46] Ma, J., Yu, H., Liu, J., Chen, Y., Wang, Q. and Xiang, L., 2015. Metformin attenuates hyperalgesia and allodynia in rats with painful diabetic neuropathy induced by streptozotocin, Eur J Pharmacol. 764, 599-606.

[47] Aschenbrenner, D.S., 2016. The FDA Revises Restrictions on Metformin Use in Kidney Impairment, Ajn the American Journal of Nursing. 116, 22-23.

[48] Yang, D., Livingston, M.J., Liu, Z., Dong, G., Zhang, M., Chen, J.K. and Dong, Z., 2018. Autophagy in diabetic kidney disease: regulation, pathological role and therapeutic potential, Cell. Mol. Life Sci. 75, 669-688.

[49] Papanicolaou, K.N., Izumiya, Y. and Walsh, K., 2008. Forkhead transcription factors and cardiovascular biology, Circ. Res. 102, 16-31.

[50] Kume, S., Koya, D., Uzu, T. and Maegawa, H., 2014. Role of nutrient-sensing signals in the pathogenesis of diabetic nephropathy, Biomed Res Int. 2014, 315494.

[51] Kitada, M., Ogura, Y., Monno, I. and Koya, D., 2017. Regulating Autophagy as a Therapeutic Target for Diabetic Nephropathy, Curr. Diab. Rep. 17, 53.

[52] Zou, J., Hong, L., Luo, C., Li, Z., Zhu, Y., Huang, T., Zhang, Y., Yuan, H., Hu, Y., Wen, T., Zhuang, W., Cai, B., Zhang, X., Huang, J. and Cheng, J., 2016. Metformin inhibits estrogen-dependent endometrial cancer cell growth by activating the AMPK-FOXO1 signal pathway, Cancer Sci. 107, 1806-1817.

Tables

Table 1 Antibody information for western blotting

Usage	Antibodies	Species	Molecular weight	Catalog	Dilutions	Manufacturer
Primary antibodies	Anti-rat pAMPKα	Rabbit	62 kDa	#4188	1:2000	Cell Signaling Technology
	Anti-rat AMPKα	Rabbit	62 kDa	#5831	1:1000	Cell Signaling Technology
	Anti-rat SIRT1	Rabbit	120 kDa	#9475	1:1000	Cell Signaling Technology
	Anti-rat pFoxO1	Rabbit	82 kDa	#9461	1:1000	Cell Signaling Technology
	Anti-rat FoxO1	Rabbit	78-82 kDa	#2880	1:1000	Cell Signaling Technology
	Anti-rat HIF1α	Mouse	132 kDa	sc-13515	1:200	Santa Cruz Biotechnology
	Anti-rat Atg12	Rabbit	16/55 kDa	#4180	1:1000	Cell Signaling Technology
	Anti-rat LC3B	Rabbit	14/16 kDa	#2775	1:1000	Cell Signaling Technology
	Anti-rat p62	Rabbit	62 kDa	#5114	1:1000	Cell Signaling Technology
	Anti-rat BECN1	Rabbit	60 kDa	#3495	1:1000	Cell Signaling Technology
	Anti-rat β-actin	Rabbit	45 kDa	#4970	1:1000	Cell Signaling Technology
Secondary antibodies	Anti-rabbit IgG-HRP	Goat	——	#7074	1:2000	Cell Signaling Technology
	Anti-mouse IgG-HRP	Horse	——	#7076	1:2000	Cell Signaling Technology

Figures

Figure 1. Flow chart.

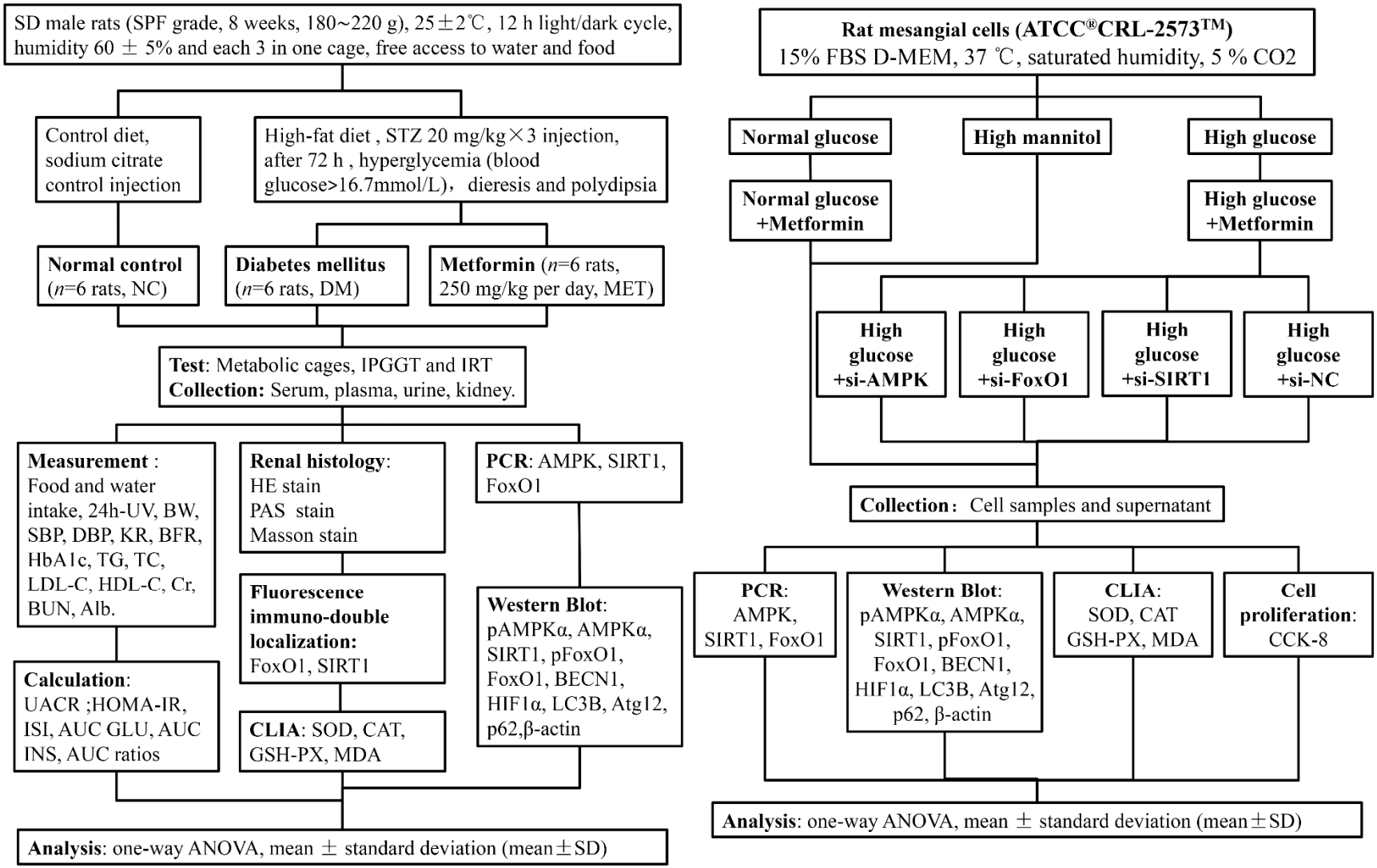

Figure 2. Changes of physiological indicators in diabetic rats treated with metformin. A) IPGTT curve, B) IRT curve, C) AUC of glucose and insulin, D) AUC ratios, E) HOMA-IR and ISI, F) HbA1c, G) SBP and DBP, H) BFR and KR, I) BW, J) TC, TG, LDL-C, HDL-C, K) Food and water intake, 24 h-UV, L) BUN and Cr, M) UACR. * Compared with the NC group, $P<0.05$. # Compared with the DM group, $P<0.05$. $n = 6$ per group.

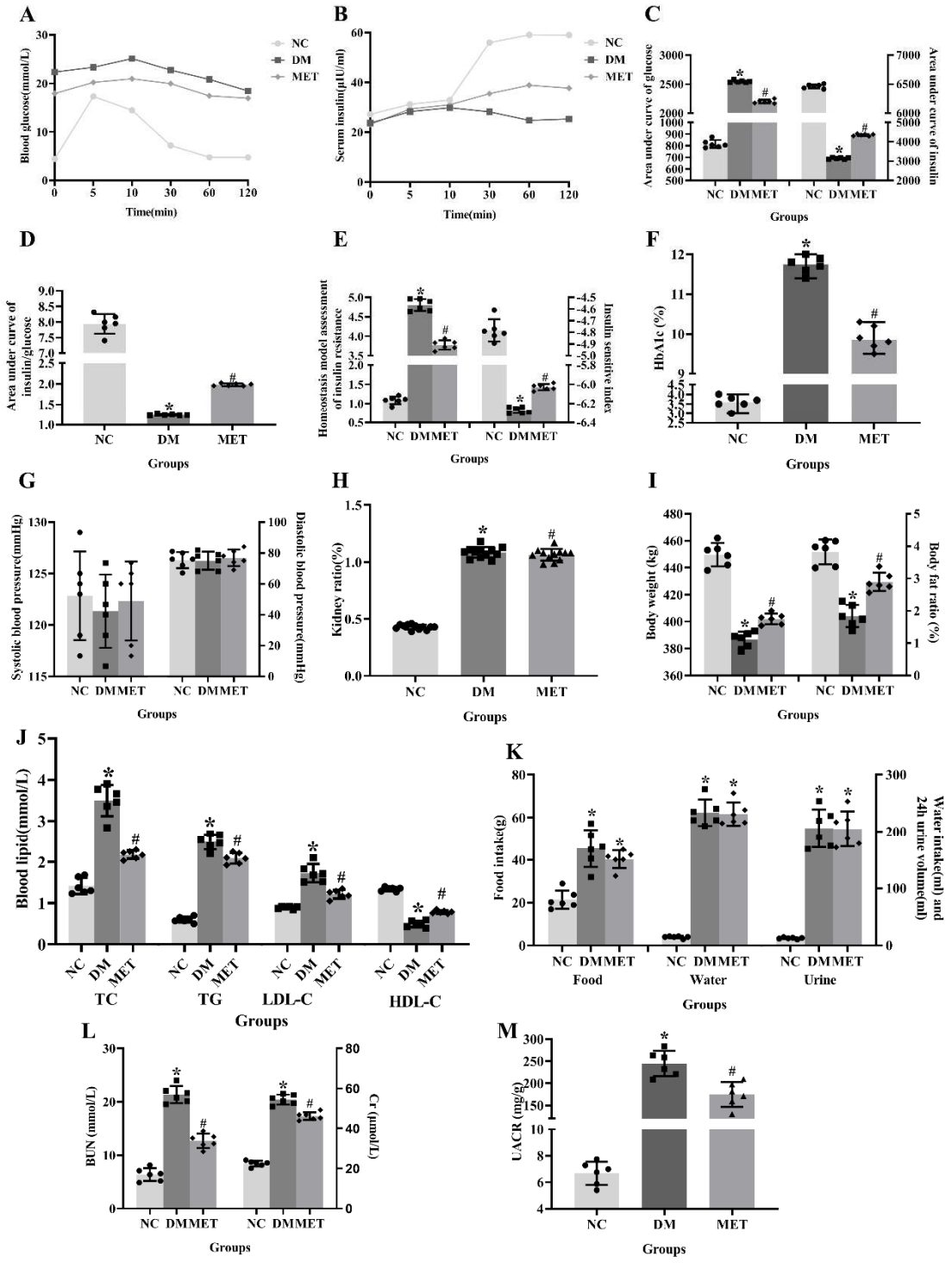

Figure 3. Renal histologic changes in diabetic rats treated with metformin. A) HE stain, B) PAS stain, C) Masson stain, Scar bar: 25 μm, D) fluorescence immune-double localization, E) Quantitative assessments of glomerular volume, mesangial expansion and fibrosis levels, F) Quantitative assessments of fluorescence immune-double localization using FoxO1/DAPI and SIRT1/DAPI. Scar bar: 50 μm. *n* = 6 per group.

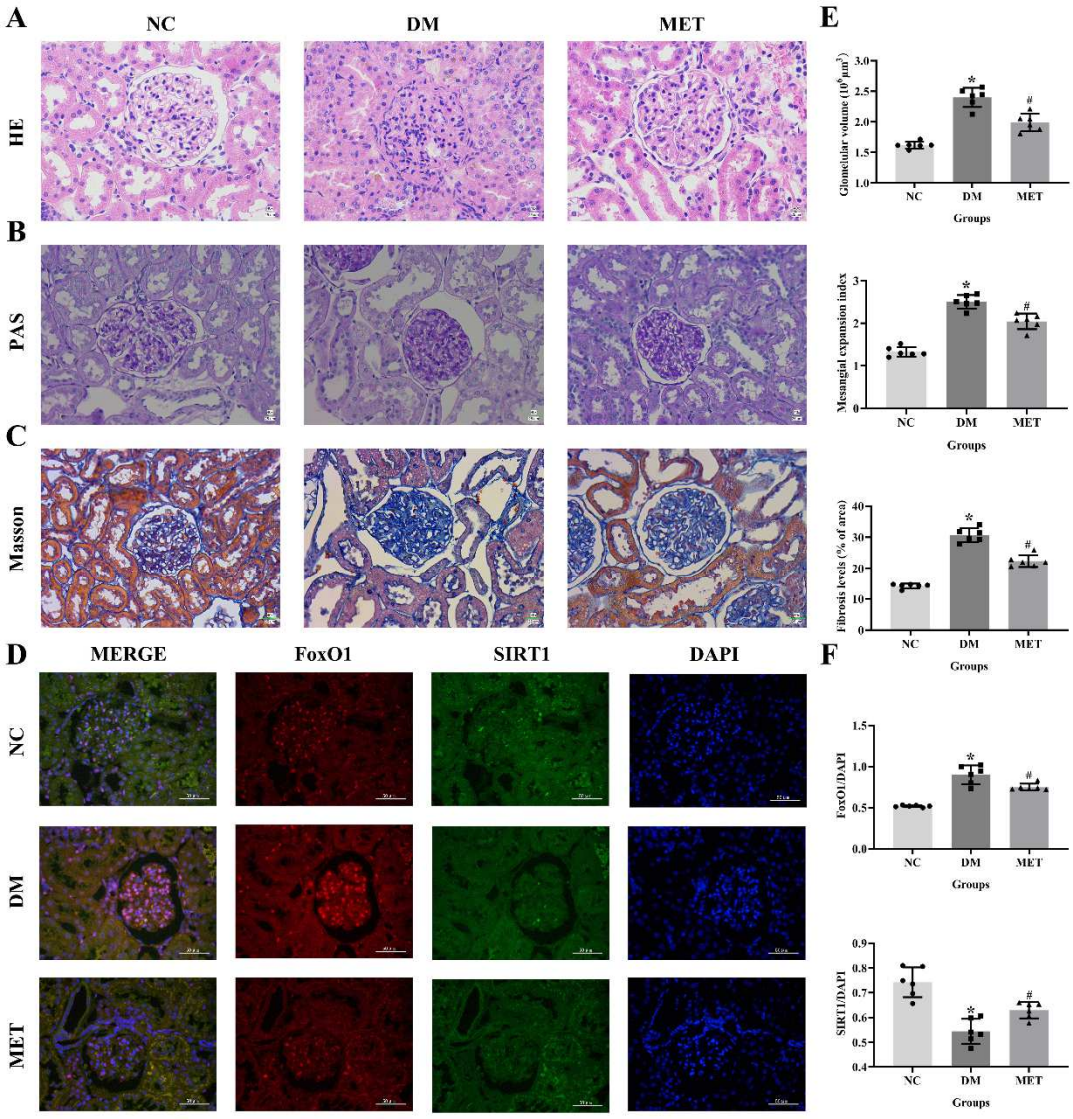

Figure 4. Renal tissue changes in diabetic rats treated with metformin. A) protein bands, B) expression levels of pAMPKα/AMPKα, SIRT1, pFoxO1/FoxO1, HIF1α, Atg12, LC3B, p62 and BECN1, C) relative expression of AMPK, SIRT1 and FoxO1 mRNA, D) levels of SOD, CAT, GSH-PX and MDA in kidney and serum. * Compared with the NC group, $P<0.05$. # Compared with the DM group, $P<0.05$. $n = 6$ per group.

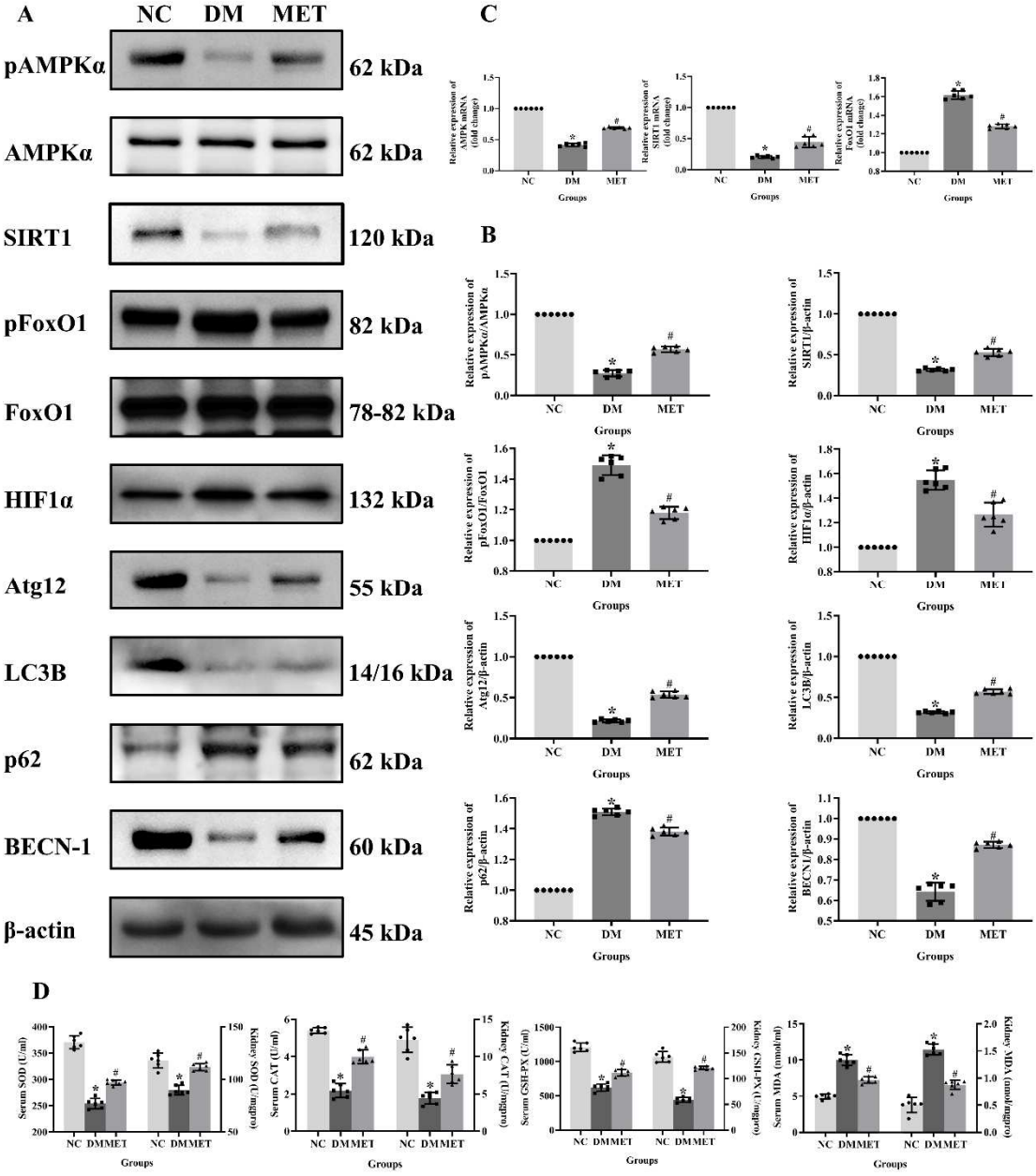

Figure 5. Changes in high glucose cultured RMCs. A) protein bands, B) expression levels of pAMPKα/AMPKα, SIRT1, pFoxO1/FoxO1, HIF1α, Atg12, LC3B, p62 and BECN1, C) relative expression of AMPK, SIRT1 and FoxO1 mRNA, D) levels of SOD, CAT, GSH-PX and MDA in cell supernatant, E) cell proliferation measured using CCK-8. * Compared with the NG group, $P<0.05$. $n = 6$ per group.

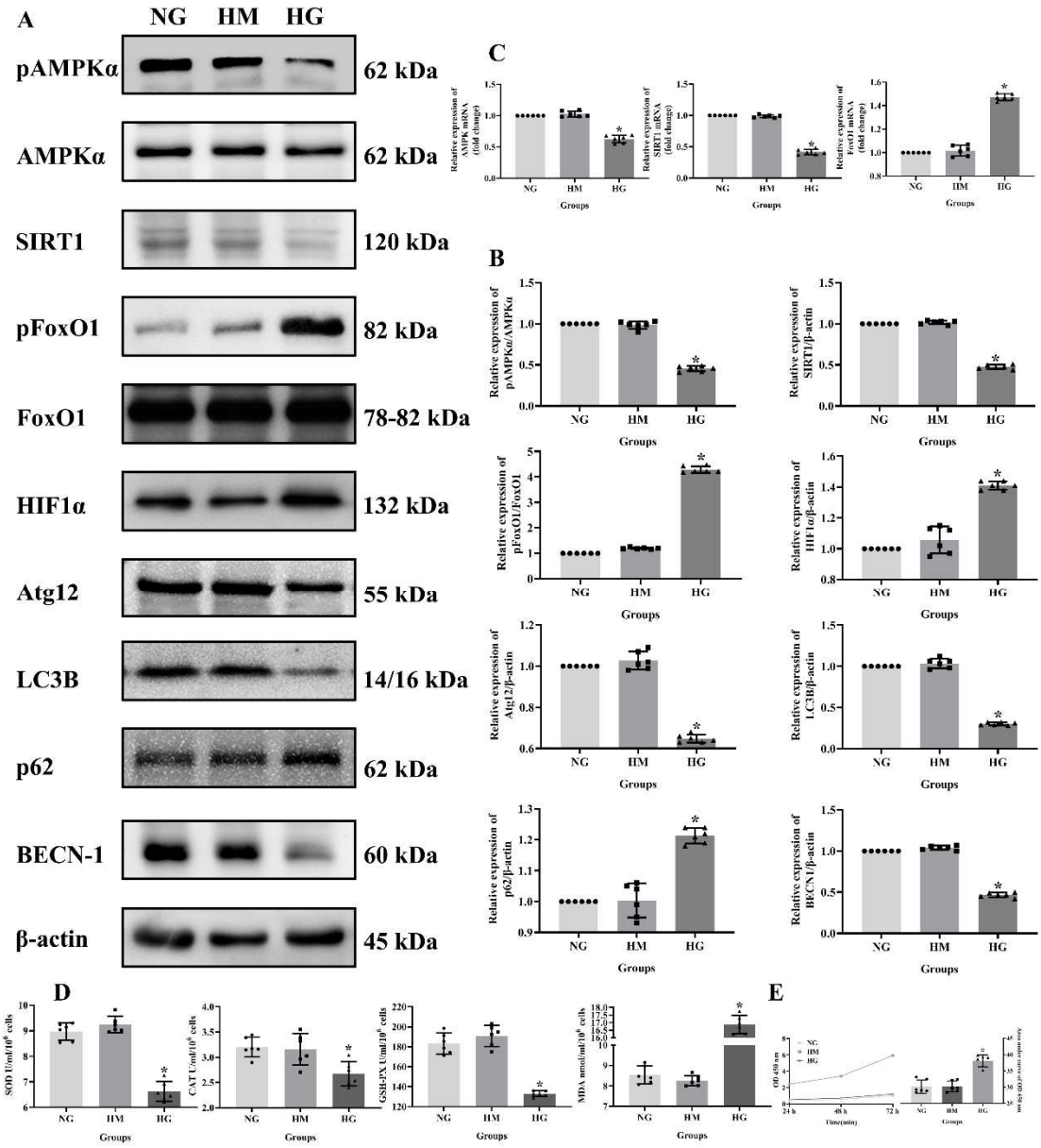

Figure 6. Effects of metformin on high glucose cultured RMCs. Proliferation of RMCs using CCK-8 A) at different concentrations of metformin, B) in normal and high glucose pre-treated with metformin, C) protein bands, D) expression levels of pAMPKα /AMPKα, SIRT1, pFoxO1/FoxO1, HIF1α, Atg12, LC3B, p62 and BECN1, E) relative expression of AMPK, SIRT1 and FoxO1 mRNA, F) levels of SOD, CAT, GSH-PX and MDA in cell supernatant. * Compared with the NG group, $P<0.05$. # Compared with the HG group, $P<0.05$. $n = 6$ per group.

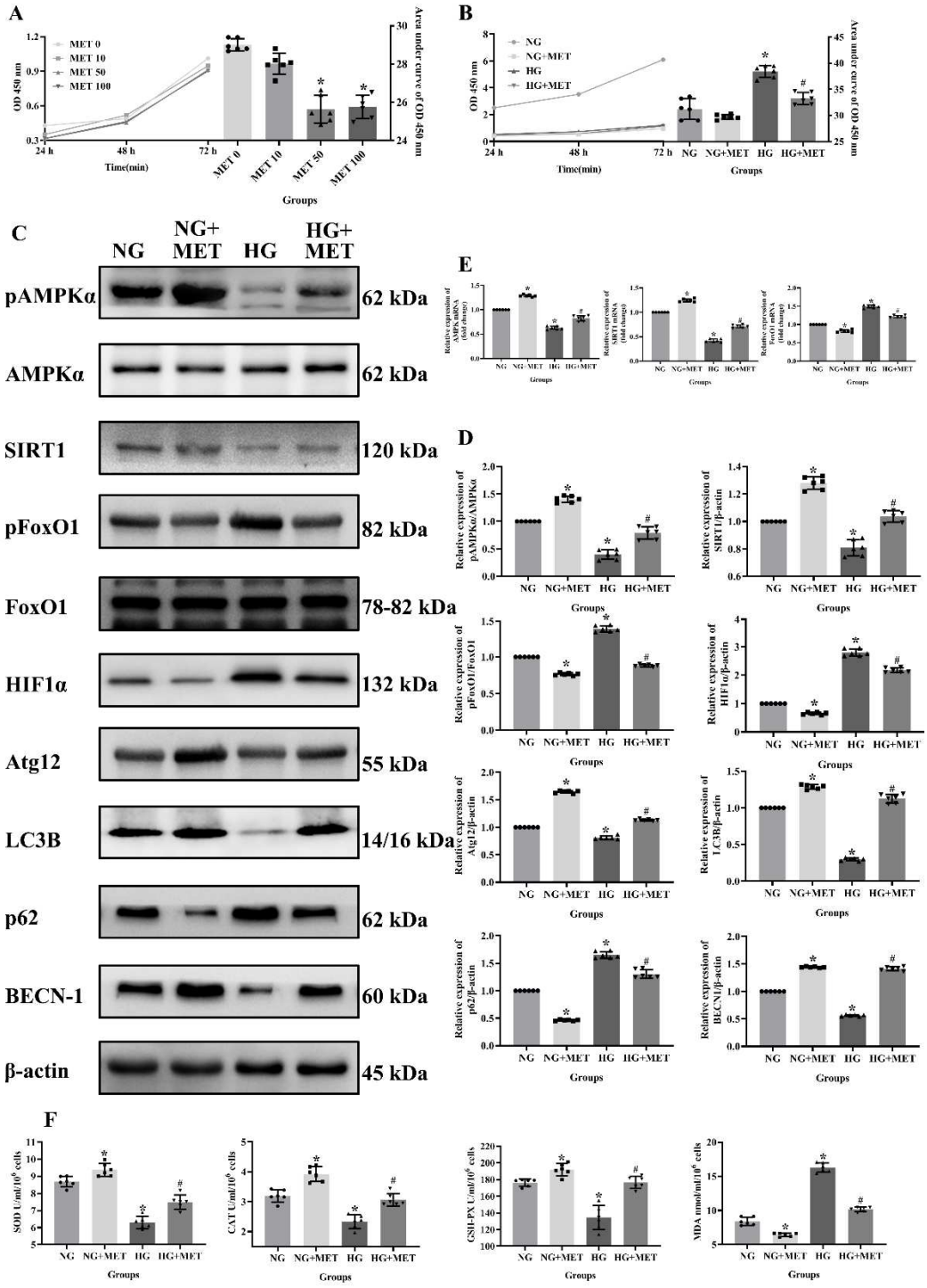

Figure 7. Changes of related factors in high glucose cultured RMCs via gene silencing of AMPK, SIRT1 and FoxO1. A) protein bands, B) expression levels of pAMPKα/AMPKα, SIRT1 and pFoxO1/FoxO1, C) relative expression of AMPK, SIRT1 and FoxO1 mRNA, D) cell proliferation measured using CCK-8. * Compared with the HG group, $P<0.05$. $n = 6$ per group.

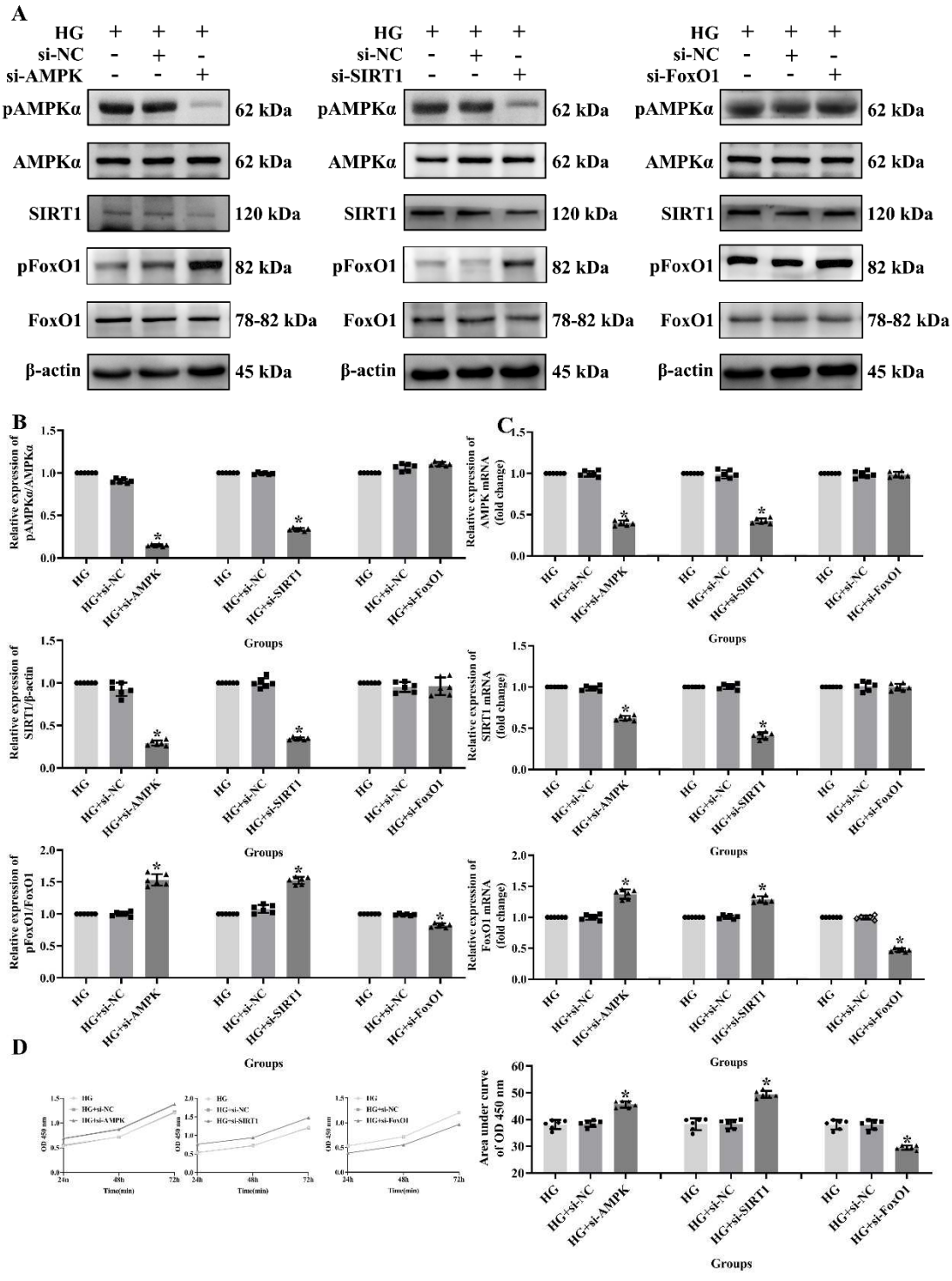

Figure 8. Possible molecular mechanisms.